Journal of Power Sources 195 (2010) 4660–4666

Contents lists available at ScienceDirect

Journal of Power Sources

journal homepage: www.elsevier.com/locate/jpowsour

Performance improvement of direct carbon fuel cell by introducing catalytic gasification process

Chen Li [a], Yixiang Shi [b], Ningsheng Cai [a,*]

[a] Key Laboratory for Thermal Science and Power Engineering of Ministry of Education, Department of Thermal Engineering, Tsinghua University, Tsinghua Yuan, Haidian District, Beijing 100084, China
[b] Institute of Nuclear and New Energy Technology, Tsinghua University, Beijing 100084, China

ARTICLE INFO

Article history:
Received 7 January 2010
Received in revised form 28 January 2010
Accepted 28 January 2010
Available online 6 February 2010

Keywords:
Direct carbon fuel cell
Catalytic gasification
Solid oxide electrolyte
Carbon
Performance

ABSTRACT

In this paper, the effects of catalytic gasification on the solid oxide electrolyte DCFC (direct carbon fuel cell) performance are experimentally investigated and analyzed using K, Ca, Ni as catalyst in carbon black and controlling the temperatures of cell and carbon black at 750 °C and 700–1000 °C, respectively. The average power densities are 976, 1473 and 1543 W m^{-2} respectively for 900, 950 and 1000 °C pure carbon black gasification. Catalytic gasification improves the DCFC performance significantly. For the same performance of pure carbon black, the gasification temperatures decrease about 200, 130 and 150 °C with K, Ca and Ni additives, respectively. The catalytic effects for carbon black gasification with CO_2 are: K > Ni > Ca. For typical identical temperature DCFC operating at 750 °C, the power densities of 0.7 V discharging are 1477, 1034 and 1123 W m^{-2} for the carbon black with K, Ca and Ni additives, respectively. It is possible to reduce the operation temperature of DCFC to the medium temperature range of solid oxide electrolyte (600–800 °C) by introducing catalytic gasification process.

© 2010 Elsevier B.V. All rights reserved.

1. Introduction

Fuel cell is one of the most promising technologies for power generation attributable to their high efficiency and few pollutants. Compared with other types of fuel cells, the direct carbon fuel cell (DCFC) represents several unique advantages, for instance, (1) the solid fuel is easy for transport and storage, and can be widely obtained from coal, coke, biomass and even wastes [1]; (2) its theoretical thermal efficiency would be up to 100% attributable to the negative entropy change in DCFC reactions [2]; (3) the conversion from carbon directly to carbon dioxide in DCFC may bring up a convenient pathway for CO_2 capture, etc.

DCFCs can be divided into three types according to their electrolytes: molten hydroxide [1,3–6], molten carbonate [7–11] and solid oxide electrolyte [12–19]. Besides, some studies have been conducted combining molten carbonate and solid oxide electrolyte to obtain better performances [20–22]. In this paper, studies were focused on the solid oxide electrolyte DCFC, which could enhance the reaction activity with higher operation temperature and could reduce the effects of liquid electrolyte consumption, leaking and corrosion, effectively.

The anode reaction mechanism of DCFC is more complex than that of gas fueled solid oxide fuel cells. Nakagawa and Ishida [12] placed charcoal in the fuel chamber of fuel cell at 1075, 1180 and 1275 K. It was supposed that the fuel cell was driven by carbon monoxide produced by the charcoal gasification. The reactions in anode are listed as following:

$$C + CO_2 \leftrightarrow 2CO \quad (1)$$

$$O^{2-} + CO \leftrightarrow CO_2 + 2e^- \quad (2)$$

Reaction (1) is the gasification reaction of carbon fuel, which is known as Boudouard reaction. Reaction (2) is the electrochemical reaction of CO, which occurs at the anode triple phase boundary (TPB). Gür and Huggins [13] placed solid carbon adjacent to an yttria-stabilized-zirconia (YSZ) tube with coated Pt electrodes, using He as the anode gas, and the temperatures of cell and carbon fuel were controlled independently. It was reported that the reactions in anode were as following:

$$2O^{2-} \leftrightarrow O_2 + 4e^- \quad (3)$$

$$C + O_2 \leftrightarrow CO_2 \quad (4)$$

or

$$2C + O_2 \leftrightarrow 2CO \quad (5)$$

Reactions (3), (4) or (5) only take place when the residual active gases are negligible in anode chamber. Liu et al. [14] developed a DCFC by approach of a conventional anode-supported tubular solid oxide fuel cell filled with commercial carbon black and the maximum power densities were 104, 75 and 47 mW cm^{-2} at 850, 800

* Corresponding author. Tel.: +86 10 62789955; fax: +86 10 62789955.
E-mail address: cains@tsinghua.edu.cn (N. Cai).

0378-7753/$ – see front matter © 2010 Elsevier B.V. All rights reserved.
doi:10.1016/j.jpowsour.2010.01.083

and 750 °C, respectively. When it was discharging, the chemical and electrochemical reactions in anode were assumed as follows:

$$C + 2O^{2-} \leftrightarrow CO_2 + 4e^- \quad (6)$$

$$C + CO_2 \leftrightarrow 2CO$$

$$O^{2-} + CO \leftrightarrow CO_2 + 2e^-$$

It was reported that the oxygen ions could react with the carbon in intimate contact with anode surface but reactions (1) and (2) were the dominant anodic reactions, which promoted the cell performance. Similarly, several other researches have been conducted by placing carbon fuel not contacting or only physical contacting with anode. In the experiments mentioned above, the carbon fuel can hardly be electrochemically oxidized by oxygen ions, which only takes place at TPB.

Ihara et al. [15–18] proposed a rechargeable direct carbon fuel cell (RDCFC), which employed a solid-carbon fuel supplied by thermal decomposition of propane. It was reported that the electrochemical oxidization of carbon occurred during power generation:

$$C + 2O^{2-} \leftrightarrow CO_2 + 4e^-$$

or

$$C + O^{2-} \leftrightarrow CO + 2e^- \quad (7)$$

Once CO was produced, it reacted with O^{2-} and DCFC operated on CO. Because the reaction rate between CO and O^{2-} in reaction (2) was expected to be higher than that of reaction (6) or (7), it was confirmed that reaction (1) took place after the production of CO_2. The CO_2 in production is often recycled to the anode again to obtain high gasification rate of carbon fuel and improve the performance of DCFC.

Therefore, the key anode reactions of DCFC are reactions (1) and (2), which dominate the performance of DCFC. For typical solid oxide electrolyte DCFC, the temperatures of button cell and carbon fuel remain the same, ranging from 600 to 1000 °C [14]. However, as reported in our previous work [23], reactions (1) and (2) depend on the temperature significantly and their optimized temperature ranges were quite different. The gasification reaction hardly took place below 800 °C and the gasification of carbon fuel was the limiting factor of DCFC performance. Meanwhile, it has become a consensus that the alkali metal, alkaline earth metal and transition metal are effective catalysts for carbon gasification [24–28], which are widely used in coal gasification research to obtain a competitive reaction rate at lower temperature.

In this paper, the catalytic gasification is adopted to accelerate the carbon gasification rate, reduce reaction temperature and thus improve the DCFC performance. Experiments have been conducted by using K, Ca, Ni as catalyst in carbon fuel and controlling the temperatures of cell and carbon fuel at 750 °C and 700–1000 °C, respectively, to analyze the effects of catalytic gasification on DCFC performance. Based on the above analysis, it can be concluded that here the "direct carbon" means using carbon as fuel directly and converting chemical energy into electricity in one chamber but not in one elementary reaction step.

2. Experimental

2.1. Testing setup

An anode-supported SOFC button cell made by SICCAS (Shanghai Institute of Ceramics Chinese Academy of Sciences) was used in this study. It consisted of a Ni/YSZ anode support layer (680 μm), a Ni/ScSZ anode active interlayer (15 μm), a ScSZ electrolyte layer (20 μm), and a lanthanum strontium manganate (LSM)/ScSZ cathode layer (15 μm) [29]. The diameter of cathode layer was 1.4 cm and diameters of other layers were all 2.6 cm. Since the button cell could be tested by using relatively simple experimental setup and have good data repeatability, it was widely used in DCFC experiments [12,15–18]. We can focus on reaction characteristics and performance analysis with negligible effects of flow distribution and heat transfer. In addition, it should be noted that the button cells were cut directly from a big cell plate. The anode and electrolyte layers of all cells were fabricated in one time, which eliminates the performance differences caused by cell to cell variations in fabrication to a certain extent. Before testing, silver paste was reticulated on the anode and cathode surface by screen-printing for current collection.

In order to analyze the effects of catalytic gasification on DCFC performance, the carbon fuel and button cell should be detached to avoid the possible electrochemical oxidization of carbon. Besides, the detachment is easy for keeping the temperatures of carbon and button cell individually, in which we can focus on the performance variation for various gasification temperatures. Fig. 1 shows the schematic of the test setup used for evaluating the performance of DCFC working at various temperatures.

The DCFC test setup consisted of the button cell, carbon fuel and other auxiliary devices. They were all enclosed in one quartz tube but heated by two furnaces separately to avoid the mutual temperature influence of carbon gasification and anodic reactions. The button cell was located at the end of two coaxial alumina tubes and impacted by an alumina plate, which was strained by springs. The Pt mesh was used as the cathode current collector and fixed to the porous cathode with silver paste screen-printed on the surface. The oxidant flowed into the inner tube to the cathode and passed through the porous Pt mesh. The porous Ni felt was fixed to the anode support layer with silver paste to collect anode current. Due to the porous structure (porosity 95%), the anode gas reached the anode easily. A borosilicate glass ring (SiO_2 76%, B_2O_3 15%, R_2O 6%, Al_2O_3 3%, Beijing Glass Instrument Factory, China) was used as sealant to separate the anode gas and cathode gas. For both anode and cathode, Pt wires were used as voltage and current probes, which connected with Pt mesh and Ni felt individually. The carbon fuel was placed in another small quartz tube under the button cell. A porous plate sintered of quartz sand was fixed in the quartz tube. Carbon fuel, quartz wool and alumina chips were placed on the plate sequentially. The small quartz tube was put into the big one and sealed from the air. The anode gas flowed into the small quartz tube, through the porous plate, carbon fuel, quartz wool, alumina chips and finally to the button cell. Here, the quartz wool and alumina chips were set to prevent the carbon fuel powder being blown away by the anode gas.

2.2. Catalyst addition and fuel preparation

Commercial carbon black (Black Pearls 2000, GP-3848, Cabot Corporation, USA) was used as fuel here and crushed to a size of 150–200 μm. The alkali metal salt K_2CO_3, alkaline earth salt $Ca(NO_3)_2{\cdot}4H_2O$, transition metal salts $Ni(NO_3)_2{\cdot}6H_2O$ were used as catalyst precursors. All chemicals used were analytical reagent grade. Here the catalysts were added by impregnation method. The addition quantities of all catalysts were set the same with a ratio of the metal atom to carbon black of 1:10 by weight. The preparation of a fuel with K, Ca or Ni additive was typical of this procedure: a sample of 0.8837 g K_2CO_3, 2.9462 g $Ca(NO_3)_2{\cdot}4H_2O$, or 2.4773 g $Ni(NO_3)_2{\cdot}6H_2O$ was added in 40 ml de-ionized water with stirring to a solution, respectively. Then 5 g air-dried carbon black sample

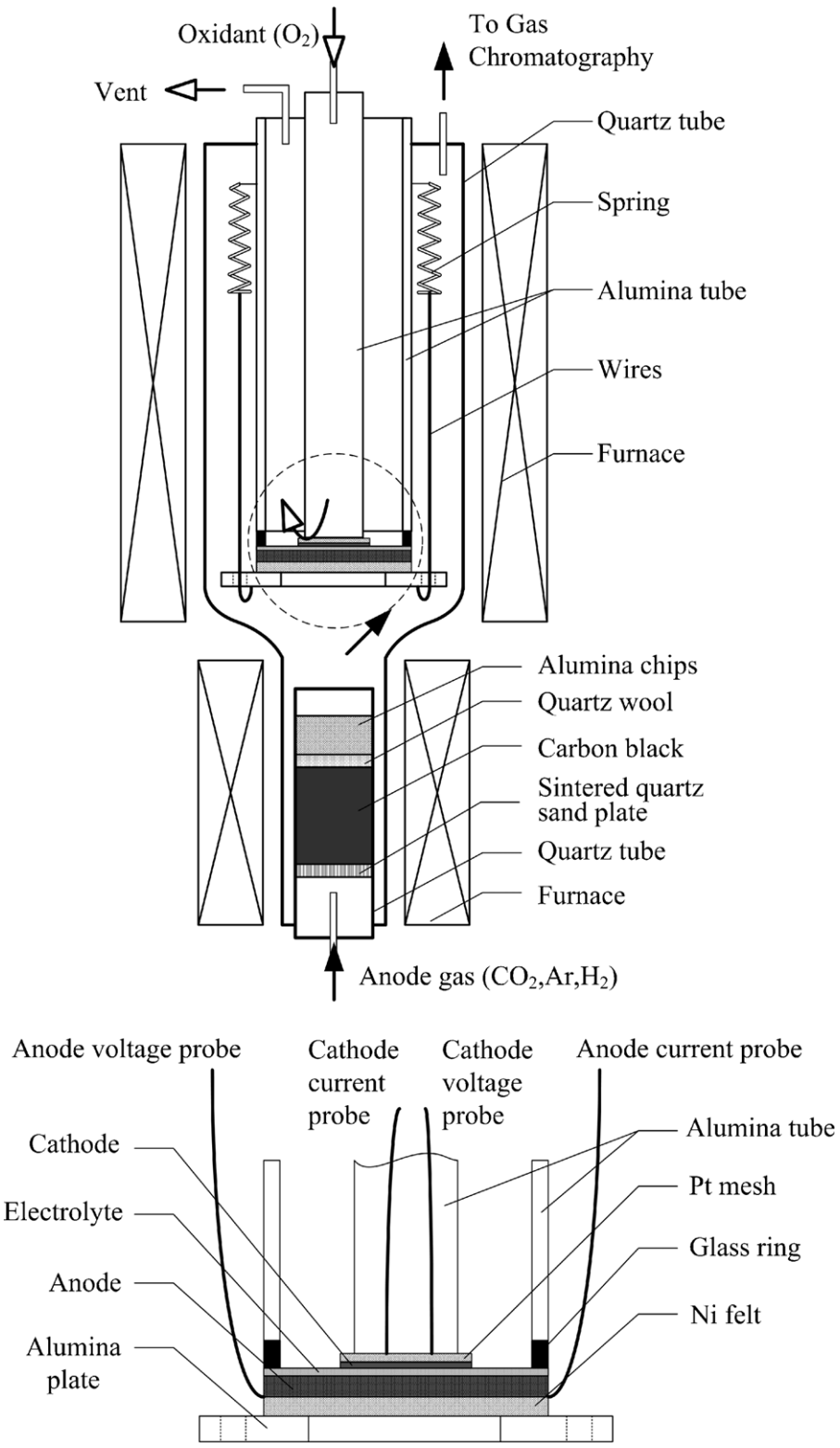

Fig. 1. Schematic of the test setup.

was added to each solution, stirred for 5 h and kept on standing in an air atmosphere for 24 h. The samples were then dried at 70 °C in oven for 24 h. After drying, each carbon black sample with additive was crushed to a size of 150–200 μm again and stored in an air-tight plastic jar. Here the pure carbon black sample and those with catalysts were assigned as "CB", "CB with K", "CB with Ca" and "CB with Ni", respectively.

2.3. Power generation experiments

Fig. 2 shows the standard procedure used in power generation experiments to characterize the DCFC performance. Before testing, the fuel sample was placed on the sintered quartz sand plate in weight of 500, 589, 705 and 656 mg for pure carbon black and the samples with K/Ca/Ni additives, respectively. All the four fuel

Before testing

Placement of carbon black and button cell

↓

Feed H_2 (50 sccm) to reduce anode for 1h, cell 750°C, carbon black ≤ 200°C

Discharge at 0.7V: electrochemical measurements and anodic gas analysis

Anode: H_2 50 sccm, cathode O_2 100 sccm, cell 750°C, carbon black ≤ 200°C

↓

Anode: CO_2 50 sccm, cathode: O_2 100 sccm, cell 750°C, carbon black ≤ 200°C

↓

Anode: CO_2 50 sccm, cathode: O_2 100 sccm, cell 750°C, carbon black 700~1000°C at an interval of 50°C

Fig. 2. Standard procedure used in power generation experiments to characterize the DCFC performance.

samples contain 500 mg carbon in theory. The temperature of button cell was kept at 750 °C while the temperature of fuel sample was kept below 200 °C in individual furnace. Pure H_2 was sent to the chamber for 1 h to reduce the anode at the flow rate of 50 ml min^{-1}. In actual testing, the DCFC was discharged at 0.7 V all the time. The constant voltage discharge curves were measured by using four-probe method with an Electrochemical Workstation IM6ex (Zahner-Elektrik GmbH, Germany). Electrochemical impedance spectra (EIS) were also performed under constant voltage of 0.7 V, with amplitude of 10 mV over the frequency from 0.1 Hz to 100 kHz. The ohmic resistance of button cell was estimated from the high frequency intercept of the impedance curve. Meanwhile, the temperature variations with elapsed time of button cell and fuel sample were recorded. Besides, the anode outlet gas was analyzed by gas chromatography (AutoSystem XL, Perkin Elmer, USA). At the beginning of testing, H_2 was used as fuel and O_2 was used as oxidant for about 0.5 h, the flow rates of which were kept 50 and 100 ml min^{-1}, respectively. Then, the anode gas was changed to CO_2 at 50 ml min^{-1}. Due to the low temperature of fuel sample (≤200 °C), it can be assumed that no reactions took place between the anode gas and carbon black here. The CO_2 was used for purging to clear the residual H_2. When the residual H_2 in anodic exhausted gas was less than 2%, the fuel sample was heated up at a heating rate about 50 °C min^{-1}. Then the carbon black temperature was kept 700–1000 °C at an interval of 50 °C, the range of which was different for the four fuel samples.

3. Results and discussion

The fuel samples used here were characterized by elemental analysis. Table 1 provides the elemental analysis results and calculated compositions of the samples. For pure carbon black, there was no obvious H and N detected in sample. The carbon content was about 94.61% and others were treated as ash. According to the stoichiometric coefficient, H_2O and metal contents of CB with Ca

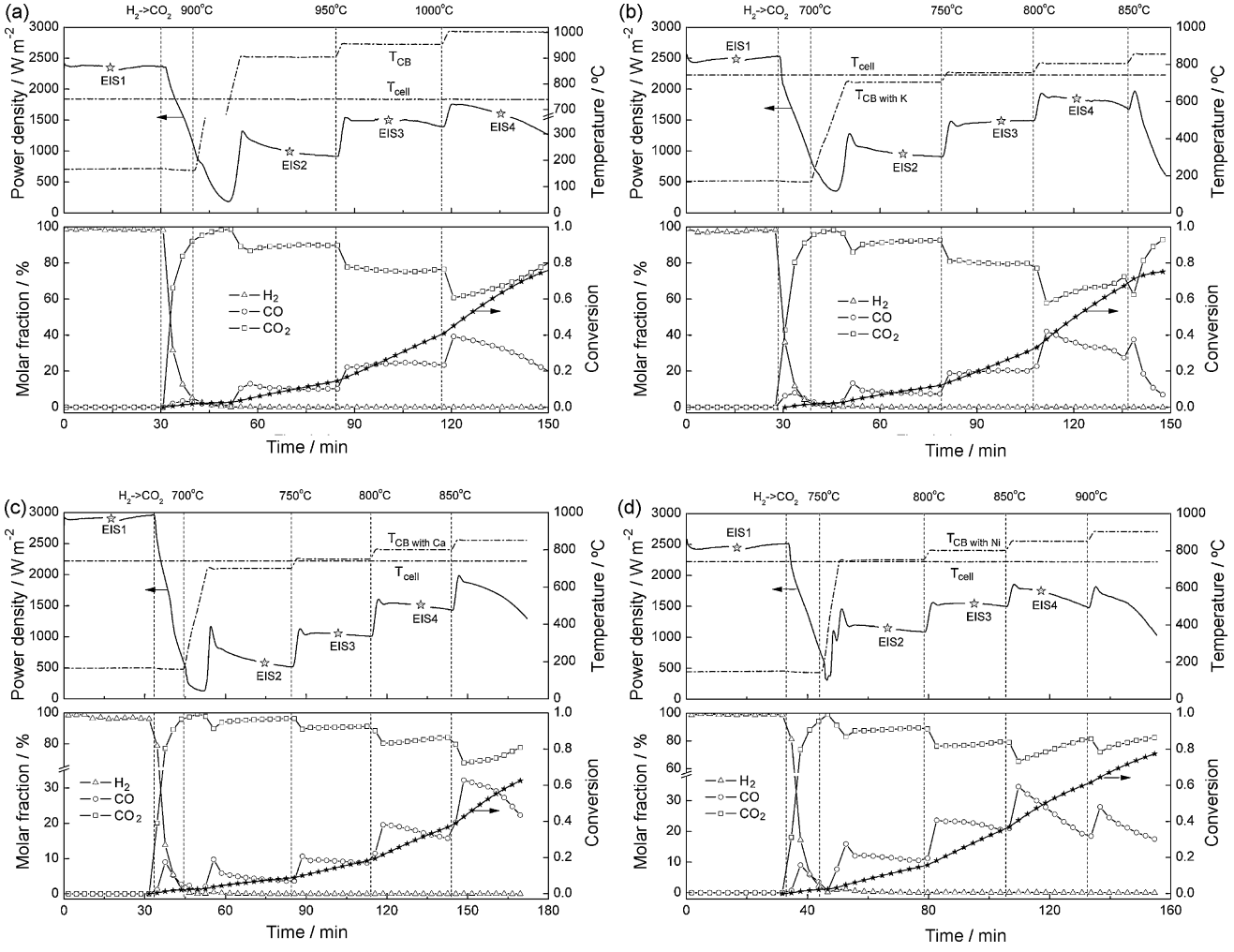

Fig. 3. Power generation characteristics of a DCFC (power density, operation temperature, anode outlet gas composition and carbon black conversion as a function of elapsed time) fueled by (a) CB, (b) CB with K, (c) CB with Ca and (d) CB with Ni.

Table 1
Elemental analysis (expressed as wt.% of the sample) and calculated compositions of carbon black samples.

Element and compositions	Measured data[a]			Calculated data				
	C (%)	H (%)	N (%)	Ash (%)	H_2O (%)	Metal (%)	M/C[b] (%)	C content (mg)
CB	94.61	<0.30	<0.30	5.39	–	–	–	472.9
CB with K	78.82	0.53	<0.30	7.75[c]	4.73	5.39	6.91	459.4
CB with Ca	63.76	0.69	3.67	8.59	6.16	5.25	8.24	449.5
CB with Ni	70.10	0.91	2.28	6.91	8.12	4.78	6.82	459.9

[a] Uncertainty for elements in carbon black <0.30%.
[b] The mass ratio of additive metal to the carbon used as fuel. Here M represents K, Ca and Ni.
[c] Determined by the average values in CB with Ca and Ni.

or Ni were calculated by the H and N elemental analysis results, respectively. Others exclude C, H_2O and additive metal salt were treated as ash. However, K content cannot be determined in the same way due to the confusion of C in carbon black and in K_2CO_3 additive. For the sake of simplicity, firstly the ash content in the CB with K was set to the average values in the CB with Ca and Ni. Then other variables can be determined. The mass ratios of additive K, Ca and Ni to carbon are 6.91, 8.24 and 6.82%, respectively. The differences of carbon content in four samples, which maybe affect the anodic gas composition and DCFC performance, are less than 3% here.

Fig. 3 shows the power generation characteristics of DCFC fueled by the four samples, including the power density (0.7 V discharging), operation temperature, anode outlet gas composition and carbon conversion as a function of elapsed time. For all the cases, the temperature of button cell was kept at 750 °C and that of fuel sample was controlled by the scheduled steps in Section 2.3. Each stage of power generation was separated by vertical dashed line and the anodic gas switchover or fuel sample temperature change step was marked on top of each figure. In each stable operation stage (no changes of temperature or anode inlet gas), the electrochemical impedance spectrum was performed under 0.7 V, which caused the gaps of power density curves and marked as stars in Fig. 3. Different from the gas fueled cell, the anodic gas composition and performance of DCFC depend on the carbon conversion significantly, which increases in the gasification process. Therefore, the performance of DCFC cannot be characterized simply by polarization curves here due to the non-steady state. The carbon conversion in Fig. 3 was calculated as follows:

$$x = \frac{0.5(m_{CO} + \Delta m_{CO_2}^{elec})}{w_0} \quad (8)$$

where x is the carbon conversion of fuel sample at a certain time t, w_0 is the total carbon content in sample, m_{CO} and $\Delta m_{CO_2}^{elec}$ are the equivalent total carbon contents of the CO in anode outlet gas and the CO_2 converted from CO by electrochemical reaction counted from start to a certain time t, respectively. Here m_{CO} and $\Delta m_{CO_2}^{elec}$ can be calculated by Simpson integration method based on the anode outlet CO flow rate and operation current at a certain time t.

Fig. 3(a) shows the power generation characteristics of the DCFC fueled by pure carbon black. In the first 30 min, the DCFC was fueled by pure hydrogen, the average power density was about 2366 W m^{-2} and no other species except H_2 was detected. Then the anode gas was changed to CO_2 to purge residual H_2, the power density and H_2 molar fraction decreased significantly. When the molar fraction of residual H_2 was less than 2%, the carbon black was heated up to 900 °C. The gasification of carbon black took place at about 800 °C and CO was produced. Due to the heating inertia, the power density and CO molar fraction overshoot at the beginning of each stable stage. The average power density (5 min later since the temperature reached equilibrium) are 976, 1473, 1543 W m^{-2} respectively for 900, 950 and 1000 °C carbon black, which are 41.3, 62.3 and 65.2% of that fueled by H_2. The corresponding average CO molar fractions are 10.3, 23.9 and 31.1%. It should be noted that the CO molar fraction at 1000 °C decreases from 39.2 to 19.4% in 30 min. The corresponding max power density for 1000 °C carbon black is 1758 W m^{-2}.

Fig. 3(b), (c) and (d) shows the similar power generation processes but at lower gasification temperatures for CB with K, Ca and Ni additives. Table 2 lists the corresponding comparisons of power density and CO molar fraction. The average power densities fueled by H_2 are 2415, 2913 and 2468 W m^{-2} for K, Ca and Ni additives, respectively. The higher power density for CB with Ca was caused by the lower ohmic resistance compared to other cells, which can be seen in Fig. 4. Here the power density ratio of the DCFC fueled by C to that fueled by H_2 was used for comparisons. For CB with K, the power density ratio and CO molar fraction are 39.6 and 7.93% at 700 °C, respectively, which are much closer to those for CB at 900 °C. Similar results are also shown in the comparisons between 750/800 °C CB with K and 950/1000 °C CB. For the same performance of pure carbon black, the gasification temperature decreases up to 200 °C for CB with K. Similarly, we can conclude that the gasification temperatures decrease about 130 and 150 °C for CB with Ca and Ni respectively, by the simple comparisons of power density ratio and linear interpolation. The catalytic effects for carbon black gasification with CO_2 are: K > Ni > Ca. Meanwhile, it should be noted that, in the power generation process, the increasing carbon conversion results in lower performance and lower CO molar fraction, which is more pronounced when the conversion is larger than 0.4 for all cases. So the comparisons here mainly focused on the low temperature stages. Due to the temperature identity for typical DCFC, here the performances at 750 °C are more concerned. The power densities of 0.7 V discharging are 1477, 1034 and 1123 W m^{-2} for CB with K, Ca and Ni at 750 °C, respectively. The optimized performance

Table 2
Comparisons of power density and CO molar fraction for the carbon black with K, Ca and Ni additives[a].

	Power density fueled by H_2 (W m^{-2})	Power density fueled by C/power density ratio[b]/CO molar fraction (W m^{-2}/%/%)			
		700 °C	750 °C	800 °C	850 °C
CB with K	2415	956/39.6/7.93	1477/61.6/19.8	1853/76.7/34.9	–
CB with Ca	2913	577/19.8/4.30	1034/35.5/9.21	1491/51.2/17.8	–
CB with Ni	2468	–	1123/45.5/11.4	1533/62.1/22.2	1630/66.0/24.7

[a] Data are all average values calculated 5 min later than the equilibrium of temperature.
[b] The power density ratio of the DCFC fueled by C to that fueled by H_2.

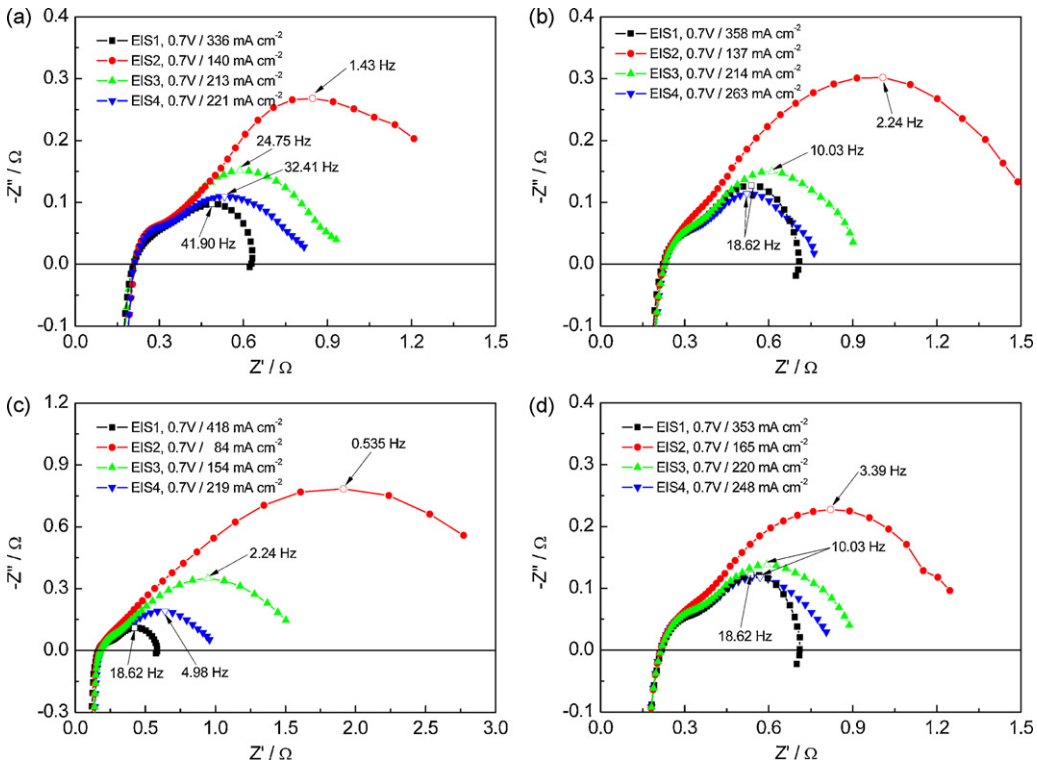

Fig. 4. Electrochemical impedance spectra of a DCFC fueled by (a) CB, (b) CB with K, (c) CB with Ca and (d) CB with Ni.

was much better than that of DCFC which used molten salt electrolyte [5–8] and solid oxide electrolyte [13–19]. By introducing catalysts gasification process, the DCFC performance is improved significantly and it is possible to reduce the operation temperature to the medium temperature range of solid oxide electrolyte (600–800 °C).

Fig. 4 shows the corresponding electrochemical impedance spectra at 0.7 V in power generation process for four fuel samples. In each figure, the ohmic resistances and the overall electrode polarization resistances were almost constant for various operation conditions due to the same cell temperature. The average ohmic resistances are 0.210, 0.226, 0.175 and 0.215 Ω for CB and CB with K, Ca and Ni, respectively. Smaller ohmic resistance for CB with Ca results in higher power density, which has been discussed earlier. Since the low-frequency arc corresponds to mass transport process, the large arcs in the low-frequency zone indicate the insufficient fuel gas in the anode. In each figure, the low-frequency arcs decrease with the increasing of carbon black temperature. Higher CO molar fraction in anode gas results in smaller mass transport resistance and higher current density.

4. Conclusions

Experiments have been performed using K, Ca, Ni as catalyst in carbon fuel and controlling the temperatures of cell and carbon fuel at 750 °C and 700–1000 °C, respectively. The DCFC performance improvements by introducing catalytic gasification have been discussed in detail based on the experimental results. For pure carbon black, the average power densities are 976, 1473 and 1543 W m^{-2} respectively for 900, 950 and 1000 °C gasification. The DCFC performance is improved significantly by introducing catalytic gasification process. For the same performance of pure carbon black, the gasification temperatures decrease about 200, 130 and 150 °C for CB with K, Ca and Ni additives, respectively. The catalytic effects for carbon black gasification with CO_2 are: K > Ni > Ca. For typical identical temperature DCFC operating at 750 °C, the power densities of 0.7 V discharging are 1477, 1034 and 1123 W m^{-2} for K, Ca and Ni additives, respectively. Therefore, the operation temperature of DCFC can be possibly reduced to the medium temperature range of solid oxide electrolyte (600–800 °C). Besides, in the power generation process, the increasing carbon conversion results in lower performance and lower CO molar fraction, which is more pronounced when the conversion is larger than 0.4.

Acknowledgements

This work is supported by the National Natural Science Foundation of China (20776078) and the Chinese High Technology Development Project (2007AA05Z151). We gratefully acknowledge the insightful discussions and offers of button cells used in experiments from Prof. Shaorong Wang in Shanghai Institute of Ceramics Chinese Academy of Sciences (SICCAS), China.

References

[1] S. Zecevic, E.M. Patton, P. Parhami, Carbon 42 (2004) 1983–1993.
[2] S. Basu, Recent Trends in Fuel Cell Science and Technology, Anamaya, New Delhi, 2007.
[3] T.A. Edison, US 460,122 (1891).
[4] W.W. Jacques, US 555,511 (1896).
[5] G.A. Hackett, J.W. Zondlo, R. Svensson, J. Power Sources 168 (2007) 111–118.
[6] T. Nunoura, K. Dowaki, C. Fushimi, S. Allen, E. Meszaros, M.J. Antal, Ind. Eng. Chem. Res. 46 (2007) 734–744.
[7] W.H.A. Peelen, M. Olivry, S.F. Au, J.D. Fehribach, K. Hemmes, J. Appl. Electrochem. 30 (2000) 1389–1395.
[8] X. Li, Z. Zhu, J. Chen, R. de Marco, A. Dicks, J. Bradley, G. Lu, J. Power Sources 186 (2009) 1–9.
[9] J.R. Selman, J. Power Sources 160 (2006) 852–857.
[10] M. Steinberg, Int. J. Hydrogen Energy 31 (2006) 405–411.
[11] J.F. Cooper, R. Krueger, N. Cherepy, US 6815105 B2 (2004).
[12] N. Nakagawa, M. Ishida, Ind. Eng. Chem. Res. 27 (1988) 1181–1185.
[13] T.M. Gür, R.A. Huggins, J. Electrochem. Soc. 139 (1992) L95–L97.
[14] R. Liu, C. Zhao, J. Li, F. Zeng, S. Wang, T. Wen, Z. Wen, J. Power Sources 195 (2010) 480–482.
[15] M. Ihara, S. Hasegawa, J. Electrochem. Soc. 153 (2006) A1544–A1546.

[16] S. Hasegawa, M. Ihara, J. Electrochem. Soc. 155 (2008) B58–B63.
[17] H. Saito, S. Hasegawa, M. Ihara, J. Electrochem. Soc. 155 (2008) B443–B447.
[18] M. Ihara, K. Matsuda, H. Sato, C. Yokoyama, Solid State Ionics 175 (2004) 51–54.
[19] S. Li, A.C. Lee, R.E. Mitchell, T.M. Gur, Solid State Ionics 179 (2008) 1549–1552.
[20] S.L. Jain, Y. Nabae, B.J. Lakeman, K.D. Pointon, J.T.S. Irvine, Solid State Ionics 179 (2008) 1417–1421.
[21] K. Pointon, B. Lakeman, J. Irvine, J. Bradley, S. Jain, J. Power Sources 162 (2006) 750–756.
[22] A.S. Lipilin, I.I. Balachov, L.H. Dubois, A. Sanjurjo, M.C. McKubre, S. Crouch-Baker, M.D. Hornbostel, F.L. Tanzclla, US 2007/0269688 A1 (2007).
[23] C. Li, Y. Shi, N. Cai, International Conference on Power Engineering 2009 (ICOPE-09), no. 2, Kobe, Japan, 2009, pp. 201–206.
[24] X. Li, C. Li, Fuel 85 (2006) 1518–1525.
[25] J. Yu, F. Tian, M.C. Chow, L.J. McKenzie, C. Li, Fuel 85 (2006) 127–133.
[26] J. Wang, K. Sakanishi, I. Saito, Energy Fuels 19 (2005) 2114–2120.
[27] G. Domazetis, J. Liesegang, B.D. James, Fuel Process. Technol. 86 (2005) 463–486.
[28] Y. Ohtsuka, K. Asami, Catal. Today 39 (1997) 111–125.
[29] Y. Shi, N. Cai, C. Li, C. Bao, E. Croiset, J. Qian, Q. Hu, S. Wang, J. Power Sources 172 (2007) 235–245.